Pergamon

PII: S0003–4878(98)00078–7

*Ann. occup. Hyg.*, Vol. 43, No. 1, pp. 67–76, 1999

Printed in Great Britain.
0003–4878/99 $19.00 + 0.00

# Modeling Breathing-Zone Concentrations of Airborne Contaminants Generated During Compressed Air Spray Painting

**MICHAEL R. FLYNN,*¶ BETTY L. GATANO,† JOHN L. McKERNAN,‡ KEVIN H. DUNN,‡ BRIAN A. BLAZICKO§ and §GARY N. CARLTON**

**Department of Environmental Sciences and Engineering, University of North Carolina, Chapel Hill, NC 27599-7400, U.S.A.; †Department of Environment and Natural Resources, PO Box 27687, Raleigh, NC 27611, U.S.A.; ‡National Institute of Occupational Safety and Health, 4676 Columbia Parkway, M/S R5, Cincinnati, OH 45226, U.S.A.; §United States Air Force Armstrong Laboratory, Industrial Hygiene Branch, Brooks Air Force Base, San Antonio, TX 78235, U.S.A.*

**This paper presents a mathematical model to predict breathing-zone concentrations of airborne contaminants generated during compressed air spray painting in cross-flow ventilated booths. The model focuses on characterizing the generation and transport of overspray mist. It extends previous work on conventional spray guns to include exposures generated by HVLP guns. Dimensional analysis and scale model wind-tunnel studies are employed using non-volatile oils, instead of paint, to produce empirical equations for estimating exposure to total mass. Results indicate that a dimensionless breathing zone concentration is a nonlinear function of the ratio of momentum flux of air from the spray gun to the momentum flux of air passing through the projected area of the worker's body. The orientation of the spraying operation within the booth is also very significant. The exposure model requires an estimate of the contaminant generation rate, which is approximated by a simple impactor model. The results represent an initial step in the construction of more realistic models capable of predicting exposure as a mathematical function of the governing parameters.** © **1999 British Occupational Hygiene Society. Published by Elsevier Science Ltd.**

*Keywords*: exposure modeling; spray-painting; ventilation; transfer efficiency; dimensional analysis

*Symbols*

| | |
|---|---|
| $A$ | area |
| $C$ | concentration |
| $D$ | breadth of worker or characteristic dimension |
| $F$ | momentum flux of air |
| $H$ | height of worker |
| $K$ | kinematic momentum flux of air, $F$ divided by ambient density |
| $M$, $m$ | mass flow rates |
| $p$ | pressure |
| $Q(z)$ | volumetric air flow carried by the spray jet at distance $z$ from nozzle |
| $U$ | average booth air velocity in the vicinity of the spraying |
| $V$ | air velocity |

*Greek symbols*

| | |
|---|---|
| $\Psi$ | the cumulative mass distribution by droplet diameter |
| $\mu$ | viscosity |
| $\rho$ | density |
| $\sigma$ | liquid surface tension |
| $\alpha$, $\beta$, $\Delta$ and $\gamma$ | constants |
| $\eta_T$ | transfer efficiency of liquid |

*Subscripts*

| | |
|---|---|
| a | air |
| atm | atmospheric conditions |
| L | liquid |
| n | at nozzle exit |
| f | at fan exit |
| o | overspray |
| p | particle |
| I | Impactor |
| sp | spray pattern |

Received 3 June 1998; in final form 28 September 1998
¶Author to whom correspondence should be addressed.

## INTRODUCTION

Currently, there are few mathematical models to provide useful predictions of worker exposure for actual industrial operations. The complex relationship between process parameters, work practices, ven-

tilation and exposure is only qualitatively defined at present. This lack of fundamental knowledge makes it difficult to optimize control interventions, as well as to make unbiased exposure estimates.

Models take different forms depending upon the objective. The intent here is to determine the functional relationship between exposure and its primary determinants, and thus provide a method to quantify the effect of alternative control interventions. The approach relies on conceptual modeling, fundamental principles of fluid mechanics and dimensional analysis. The strategy is to define the generation rate of contaminant available for exposure and to characterize the air velocity field that transports the contaminant to the breathing zone. Scale model wind-tunnel experiments are employed to estimate the form of the mathematical relationship between breathing-zone concentration and the independent variables.

The application of paints and coatings by compressed air atomization is cost-effective and widespread. Pigments and volatile solvents are the main hygienic concern. Application is generally accomplished with either a conventional (high pressure) or an HVLP (high-volume low-pressure) spray gun. Due to the strong momentum flux of air from these guns (high velocities and pressures), control of exposure is difficult. Although spray painting generally takes place in ventilated booths, workers must often wear respiratory protection. The specific task selected for modeling is the spray painting of a flat plate in either of two orientations within a cross-flow spray-booth (see Fig. 1).

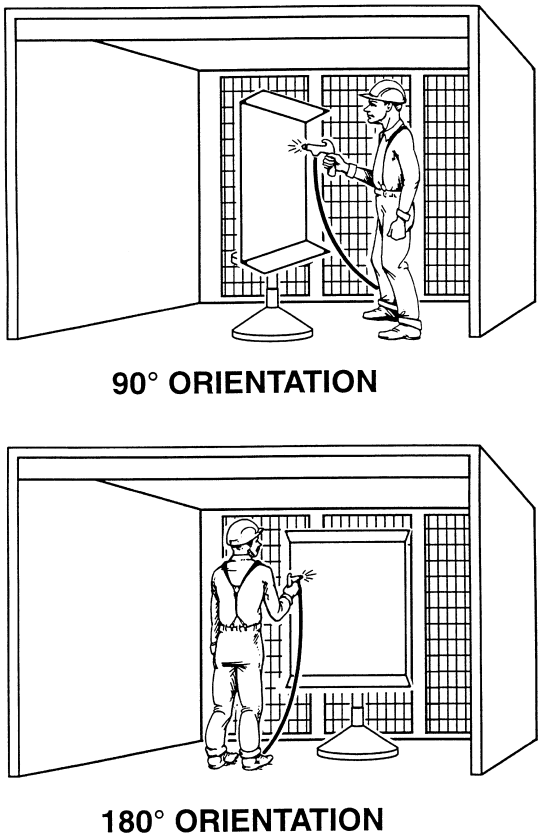


Fig. 1. Compressed air spray painting in a cross flow booth—two distinct orientations.

Spray painting is a sequence of related processes: (1) the atomization of paint (2) the transfer efficiency of paint to the work piece with subsequent over-spray generation and (3) the exposure of the worker to the over-spray (Carlton and Flynn, 1997a). The transfer of paint to the work piece is an impaction process, where the atomized droplets are transported by an airflow similar to a free turbulent jet. This jet provides the droplets with the momentum necessary to impact on the work piece. Particles with insufficient momentum escape as overspray. The subsequent transport of mist to the breathing zone is governed by the interaction of the air jet, the booth airflow and the geometry of objects within the booth, i.e., the worker and work piece being painted.

## MODEL DEVELOPMENT

The three processes of atomization, contaminant generation and exposure, are the basis for the modeling work. Each is addressed in detail below.

*Atomization*

For most spray-paint nozzles, atomization is accomplished by surrounding a circular liquid orifice with a co-axial annulus for air. The parallel flow of the two fluids results in atomization and the generation of a droplet size distribution. Supplementary atomization air may be introduced through additional holes in the air cap as well. Fan air, discharged from opposing air-horns, is used to shape the spray into an elliptical pattern. Air cap pressure is generally less than 69 kPa gauge (10 psig) for HVLP guns and greater than 276 kPa gauge (40 psig) for conventional guns. This demarcation is significant since studies show that atomization with pressures less than a critical value produce notably larger droplet sizes (Tsai and Viers, 1992). This threshold pressure is very close to the value needed to produce sonic flow through the orifice, i.e., about 89–97 kPa gauge (13–14 psig). The higher transfer efficiency associated with HVLP guns appears to be related to this increased droplet size and the associated improvement in impaction.

In this work, all droplet size distributions are estimated from empirical investigations (Kim and Marshall, 1971) which examined the co-axial air-blast atomization typical of spray guns. The cumulative mass size distribution of droplets is:

$$\Psi = \frac{1.15}{1 + 6.67\exp(-2.18d^*)} - 0.15, \qquad (1)$$

where:

$$d^* = d/MMD. \qquad (2)$$

Here, $d$ is a given droplet diameter. $MMD$ is the mass median diameter (in μm) and is calculated for air to liquid mass flow ratios less than 3 as:

$$MMD = \left\{5117\left(\frac{\sigma^{0.41}\mu_L^{0.32}}{[v^2\rho_n]^{0.57}A^{0.36}\rho_L^{0.16}}\right) + 18905\left(\left[\frac{\mu_L^2}{\rho_L\sigma}\right]^{0.17}\left[\frac{M_L}{M_a}\right]\frac{1}{v^{0.54}}\right)\right\}, \quad (3)$$

where:

| | |
|---|---|
| $\rho_n$ | air density at the nozzle (g/cc), |
| $\rho_L$ | liquid density (g/cc), |
| $\sigma$ | liquid surface tension (dynes/cm), |
| $v$ | relative velocity of air and liquid (cm/s), |
| $\mu_L$ | liquid viscosity (poise), |
| $A$ | nozzle area for atomization-air flow (sq.cm) |
| $M_L/M_a$ | ratio of liquid to atomization-air mass flows. |

It is assumed that liquid and particle densities are identical and uniform over all droplet sizes. The relative velocity of the air and liquid is taken simply as the air velocity at the atomization-air annulus, $V_n$. The area, $A$, and the mass flow rate of air, $M_a$, as used in eq. (3) apply to the atomization air only; i.e., they do not include the fan air or the area of the fan air discharge. These restrictions are consistent with the nozzle-types investigated by Kim and Marshall (1971) and are needed to distinguish between the atomization process and shaping the spray pattern. These equations have been used in previous studies (Kwok, 1991) to model spray painting droplet size distributions.

*Contaminant generation and transfer efficiency*

To develop a model of contaminant generation rate and transfer efficiency, it is assumed that the essential process dynamics can be simulated by an imaginary impactor with either a circular or rectangular orifice depending upon whether the spray pattern is circular (fan air off) or elliptical (fan air on). The characteristic dimension of this 'impactor' ($D_I$), is determined from the following geometric simplification: (1) the spray pattern is either a circle or ellipse with a diameter or width (short dimension of the elliptical spray pattern) of ($D_{sp}$), (2) the spray-gun is considered a free-jet source of momentum at a distance, $z_t$, from the plate and (3) the imaginary impactor is at a distance of ($\beta D_I$), from the plate being sprayed where $\beta$ is either 1.0 for a circular pattern or 1.5 for an elliptical spray pattern (Hinds, 1982).

Figure 2 illustrates this imaginary impactor geometry. Through trigonometry, $D_I$ is determined as:

$$D_I = \frac{z_t D_{sp}}{\beta D_{sp} + z_t}. \quad (4)$$

The air velocity through this 'impactor' is calculated using a simple air entrainment model, assuming the spray gun generates an air flow pattern similar to that of an equivalent-momentum free jet. The droplet size

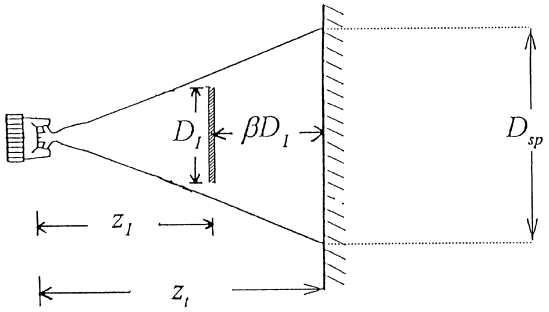

Fig. 2. Impaction model for spray painting.

distribution created by the spray gun is calculated from eq. (1). A step function cut is assumed using a critical Stokes number of 0.22 for a circular pattern and 0.53 for an elliptical pattern (Hinds, 1982). All the mass in droplets larger than the cut size is assumed to impact on the plate, while all the mass in smaller sizes is assumed to become overspray.

Transfer efficiency, ($\eta_T$) is defined here as the fraction of the liquid flow rate ($m_L$) that deposits on the work piece. The contaminant overspray generation rate ($m_o$) is:

$$m_o = (1-\eta_T)m_L. \quad (5)$$

Transfer efficiency is 1 minus the integral of the mass distribution, up to the cut diameter; thus,

$$\eta_T = 1 - \Psi(d_{50}). \quad (6)$$

To calculate transfer efficiency, $d^*$ is evaluated at $d = d_{50}$. Assuming the Cunningham correction factor is one, (reasonable for large droplets), the cut diameter (in μm) is (Hinds, 1982):

$$d_{50} = 10000\sqrt{\frac{9(Stk)\mu D_I}{\rho_p V_I}}, \quad (7)$$

where:

| | |
|---|---|
| $V_I$ | impactor air velocity (cm/s), |
| $D_I$ | imaginary impactor dimension (cm), |
| $\mu$ | air viscosity (poise), |
| $Stk$ | the critical Stokes number (0.22 or 0.53) |
| $\rho_p$ | the particle density (g/cc). |

As indicated in Fig. 2, the imaginary impactor is located at a distance $z_I$ from the spray gun, where $z_I = z_t - \beta D_I$. The average air velocity through this impactor, $V_I$ in eq. (7), is determined by:

$$V_I = \frac{Q(z=z_I)}{A_{jet}(z=z_I)}. \quad (8)$$

Here, $Q(z=z_I)$ is the volumetric airflow carried by the jet at $z_I$ including entrainment and $A_{jet}(z=z_I)$ is the cross sectional area of the air jet which is carrying droplets. The total airflow is based on a simple revision to a classic axi-symmetric entrainment model (Schlichting, 1979):

$$Q(z=z_1)=0.404 z_1\sqrt{K}, \tag{9}$$

where

$$K=\frac{\rho_n A_n V_n^2+(p_n-p_{atm})A_n}{\rho_{atm}}+\frac{\rho_f A_f V_f^2+(p_f-p_{atm})A_f}{\rho_{atm}} \tag{10}$$

is the kinematic momentum flux, $p$ is pressure and

$$A_{jet}=\pi z_f^2 \tan^2(14.5^\circ). \tag{11}$$

In eq. (10), the n and f subscripts distinguish the nozzle atomization air and fan air flows, respectively; this indicates that it is the combined momentum flux of both air sources which contributes to the transport of the droplets to the plate. This is in contrast to eq. (3), where the atomization air alone determines the size distribution. In the cases examined here, the two right-hand terms in eq. (10) are approximately equal. The inclusion of the pressure difference terms in eq. (10) reflects the contribution to momentum when air velocities are sonic, mass flow is choked and nozzle/fan exit pressure is greater than atmospheric pressure (Abramovich, 1963). For all subsonic (e.g., HVLP) nozzles, the pressure difference terms are zero. In eq. (11), it is assumed that the airflow is passing through an area expanding at an included angle of 29 degrees (Baturin, 1972).

Through the use of these equations, it is possible to estimate the generation rate of contaminant for use in the exposure model presented below. The model predicts the fraction of liquid that deposits on the plate and, hence, the mass generation rate available for exposure. The theoretical treatment is based on a liquid of low volatility, i.e., where evaporation is negligible. For most paints and coatings, this is not true and a significant fraction of the material sprayed will evaporate. The question of when such evaporation occurs and the effect this phase partitioning has on both exposure and contaminant generation models is a focus of current research.

*Contaminant transport and exposure*

The question of modeling contaminant transport and exposure, once the generation rate is known (measured), was addressed in the original model (Carlton and Flynn, 1997a) for the case shown in Fig. 1. Dimensional analysis provided the following model statement in functional form:

$$\frac{CUHD}{m_o}=\Phi\left(\frac{m_a}{m_L}, \frac{p_n H}{\mu_l U}, \text{orientation}\right), \tag{12}$$

where:

$C$ is the total mass concentration in the breathing zone,
$U$ is the average air velocity in the cross-flow spray-booth (assumed uniform),
$H$ and $D$ are the height and breadth of the worker,
$m_o$ is the overspray generation rate,
$m_a$ and $m_L$ are mass flows of air and liquid, respectively, from the spray gun,
$p_n$ is the air cap pressure and
$\mu_L$ is the liquid viscosity.

Equation (12) indicates that a dimensionless breathing zone concentration should be a function of the air to liquid mass flow ratio, a dimensionless nozzle-pressure and the orientation of the worker and spray gun within the cross-flow booth. It does not specify the form of the function, which must be deduced from experimental data. Based on scale-model wind tunnel experiments using a mannequin and a sonic nozzle (1/4 J Spray Systems Inc.) similar to a conventional spray gun, the data shown in Fig. 3 were obtained. From these data, it was determined that the mass flow ratio of air to liquid was not significant. Two equations were developed, one for each orientation, to provide a simple quantitative model (Carlton and Flynn, 1997a).

In a field evaluation of this model, eight workers were sampled for total mass (particulate and vapor) for 55 separate spray painting tasks. Four of the eight workers had predicted mean exposures within one standard error of the measured mean (Carlton and Flynn, 1997b). The overall predicted mean exposure, based on all 55 tasks, was within one standard error of the measured overall mean. In summary, the original model seemed to hold promise for predicting the total mass exposure from conventional spray painting in cross-flow booths when the overspray generation rate was known and where the geometry of the work piece was reasonably approximated as a flat plate.

Although the original model worked well, the interpretation of the dimensionless pressure term was problematic because it combined the viscosity of the liquid with the air pressure of the nozzle. In addition, it became clear from further studies (McKernan, 1997; Dunn, 1997) that the curve shown in Fig. 3 was inadequate to characterize exposures from HVLP spray guns. Similar curves were observed, but at much lower values for the dimensionless pressure variable. This suggested that the original dimensional analysis was not general enough to incorporate the differences between HVLP and conventional spray guns. Since HVLP guns operate at lower pressures than conventional guns, and these pressures no longer produce sonic velocities, a primary assumption in the original model was violated.

To account for this, a revised dimensional analysis using the ratio of the spray gun momentum flux ($F_g$) to the momentum flux through the projected area of the mannequin ($F_m$) was employed. Previous work (Kim and Flynn, 1992), had illustrated that this ratio was important in explaining tracer gas concentrations generated by sources with significant momentum. This ratio can be defined with reference to eq. (10) as:

$$\frac{F_g}{F_m}=\frac{K}{HDU^2}. \tag{13}$$

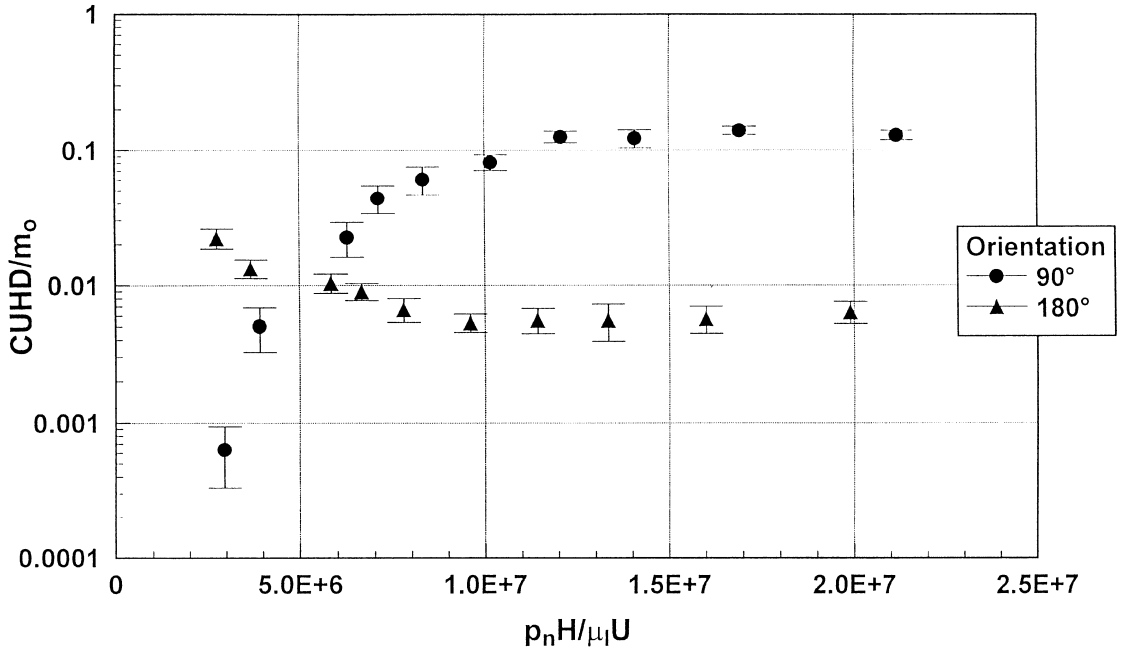


Fig. 3. Experimental results for 1/4 J nozzle: dimensionless breathing zone concentration as a function of dimensionless pressure variable, by orientation.

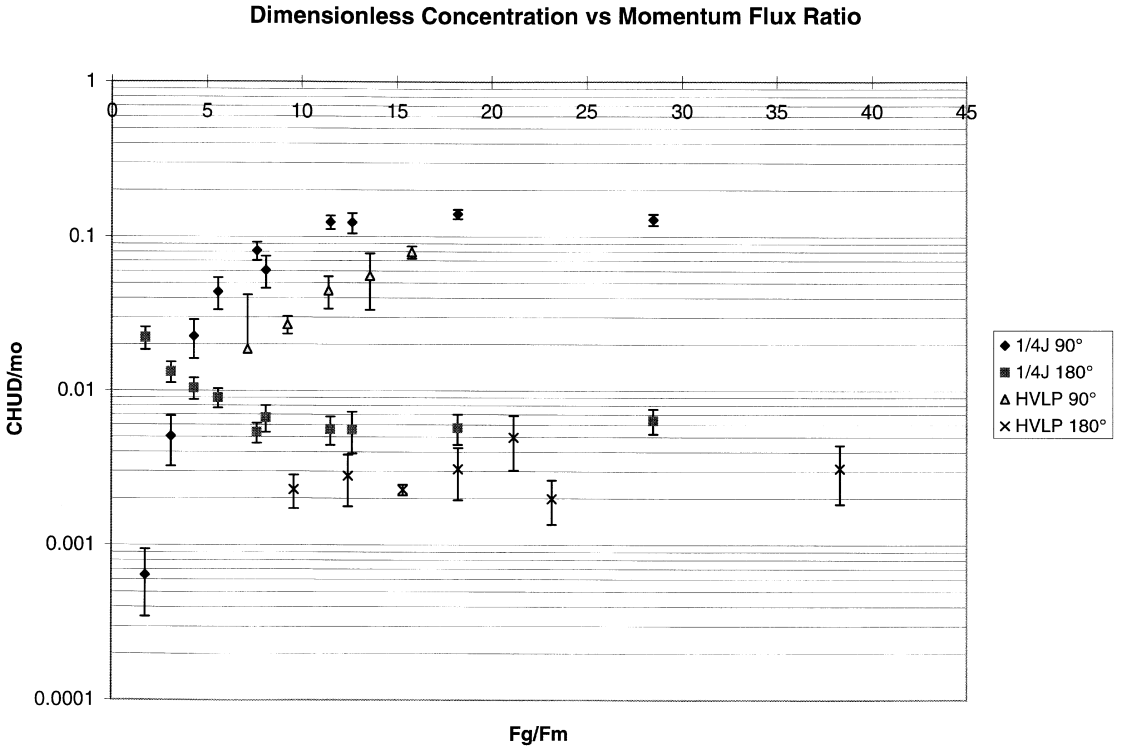


Fig. 4. Experimental results for both 1/4 J and HVLP: dimensionless breathing zone concentration as a function of momentum flux ratio, by orientation.

When this momentum flux ratio replaces the original dimensionless pressure variable, the 1/4 J data shown in Fig. 4 result. Equation (14) and eq. (15) were fitted to the 1/4 J data by estimating the asymptotes graphically and conducting linear regressions on appropriate log transforms of the variables; values of $r^2 = 0.88$ were obtained for both orientations. These equations define the revised exposure model,

$$\log_{10}\left(\frac{CHUD}{m_o}\right)_{90} = -0.796 - 5.37\left(\frac{F_g}{F_m}\right)^{-1.58} \quad (14)$$

and

$$\log_{10}\left(\frac{CHUD}{m_o}\right)_{180} = -2.3 + 0.8\left(\frac{F_g}{F_m}\right)^{-1}. \quad (15)$$

Liquid viscosity is no longer included in this portion of the dimensional analysis. The properties of the liquid enter the model only through their impact on the overspray generation rate.

The experimental work and analysis described below is designed: (1) to examine the model outlined above for transfer efficiency eq. (6), and (2) to determine whether the revised exposure model (Equation (14) and eq. (15)) is applicable to HVLP guns.

## METHODS

The experimental data were taken from 2 studies identified here as A and B. Study A (Carlton and Flynn, 1997a) employed the sonic 1/4 J nozzle, in a 1.5 m square wind tunnel, with a 1.04 m tall by 20 cm wide mannequin. Air velocities ranged from 0.25–0.78 m/s (50–150 fpm) in the wind tunnel. Study B (Gatano, 1997; Blazicko, 1998) used a subsonic DeVilbiss MSV-533-4-FF HVLP spray gun and full-size mannequin 1.83 m (72 in) tall and 36 cm (14 in) across the chest. Study B exposure data were collected in an actual spray-booth, 2.21 m by 1.91 m (87 in by 75 in), with air velocities ranging from 0.25–0.62 m/s (50–120 fpm). Study A used corn oil to represent the paint while a non-volatile vacuum pump oil was used in Study B. Table 1 lists the relevant dimensions for both studies.

Similar air sampling methods were used in both studies. PVC membrane filters were located in the 'breathing zone' of the mannequins. In study A, an open faced 37 mm cassette was used, while in study B, a cassette with a 25 mm inlet was used and mounted in a holder designed to keep the face of the cassette parallel to the body. All filters were weighed on an electro-balance with 0.001 mg sensitivity. At least 1.0 mg of mass was collected for each sample. The air flow through the filter was 2.0 l/min in both studies.

In each study, transfer efficiency was determined by mass balance. The amount of liquid sprayed was measured and the amount deposited on the plate was weighed after being carefully removed with a rubber scraper. Nozzle pressures and mass flow rates of both air and liquid were also measured directly. The isentropic flow equations (White, 1986) were used to calculate air density and velocities at both nozzle and fan exits to determine the needed momentum fluxes. Table 2, Table 3 and Table 4 provide, respectively, the geometric, liquid and nozzle properties pertinent to the models.

## RESULTS

The HVLP dimensionless exposures of study B are plotted in Fig. 4, along with the 1/4 J data discussed previously. Although there is a clear difference between the two data sets, the results and trends are similar. Spray-booth limitations prevented an examination of HVLP exposures over a range of momentum ratios comparable to study A, particularly in the side orientation. The full curve, including the plateau region of constant dimensionless concentration observed with the sonic nozzle, was not achieved.

The dimensionless concentration tends to be greater in the 90 degree orientation than in the 180 degree orientation over momentum flux ratios typical of most real spray operations. This is related to the deflection of the spray upstream by the plate, with subsequent recirculation to the worker, as has been observed in field studies (Heitbrink et al., 1994) and in the laboratory (Carlton and Flynn, 1997a). The crossover point of the exposure curves is consistent with previous studies, indicating the superiority of the side orientation for passive and low momentum sources.

Comparisons between measured and predicted transfer efficiencies for studies A and B are given in Fig. 5 and Fig. 6, respectively. The agreement depends on nozzle type. As Fig. 5 shows, the agreement between predicted and measured transfer efficiency for the 1/4 J nozzle depended upon nozzle pressure. The data from study A cluster along the $x$-axis in three

Table 1. Approximate experimental dimensions

| | Study A 1/4 J (m) | Study B HVLP (m) |
|---|---|---|
| Mannequin height ($H$) | 1.04 | 1.85 |
| Mannequin breadth ($D$) | 0.20 | 0.36 |
| Wind tunnel or booth width | 1.52 | 1.91 |
| Wind tunnel or booth height | 1.52 | 2.21 |
| Plate width | 0.66 | 1.07 |
| Plate height | 1.02 | 1.52 |
| Length of mannequin arm | 0.08 | 0.43 |
| Distance from nozzle to plate | 0.20 | 0.20 |

1/4 J = Spray Systems Inc. spray nozzle; HVLP = DeVilbiss MSV-533-4-FF spray gun.

Table 2. Imaginary impactor geometrical data

| Study (nozzle type) | $Z_t$ (cm) | $D_{sp}$ (cm) | $D_I$ (cm) | $Z_I$ (cm) | $Stk(50)$ |
|---|---|---|---|---|---|
| A (1/4 J) | 20.3 | 6.4 | 4.9 | 15.4 | 0.22 |
| B (HVLP) | 20.3 | 11.4 | 6.2 | 14.1 | 0.53 |

$Z_t$ = the nozzle-to-plate distance; $D_{sp}$ = the spray pattern dimension; $D_I$ = the characteristic impactor dimension; $Z_I$ = the nozzle-to-impactor distance; $Stk(50)$ = the critical Stokes number.

Table 3. Liquid properties

| Study (nozzle type) | Liquid | Density (g/cc) | Viscosity (cp) | Surface tension (dynes/cm) | Liquid mass flow rate (g/min) |
|---|---|---|---|---|---|
| A (1/4 J) | corn oil | 0.91 | 40–57 | 32.5 | 49–177 |
| B (HVLP) | vacuum pump oil | 0.86 | 68–93 | 40.5 | 79–139 |

Table 4. Nozzle properties

| Study I.D. (nozzle type) | Nozzle pressure (kPa) | Total mass flow of air (g/s) | Nozzle velocity (m/s) | $M_a/M_L$ ratios (cap air only) | $K$ ($m^4/s^2$) |
|---|---|---|---|---|---|
| A (1/4 J) | 138–345 | 1.06–2.05 | 356–389 | 0.7–1.3 | 0.37–0.86 |
| B (HVLP) | 10.4–44.9 | 3.58–9.07 | 129–255 | 0.9–2.4 | 0.45–1.9 |

$M_a$ = the mass flow rate of air; $M_L$ = the mass flow rate of liquid; $K$ = the kinematic momentum flux of air, including fan air, if present.

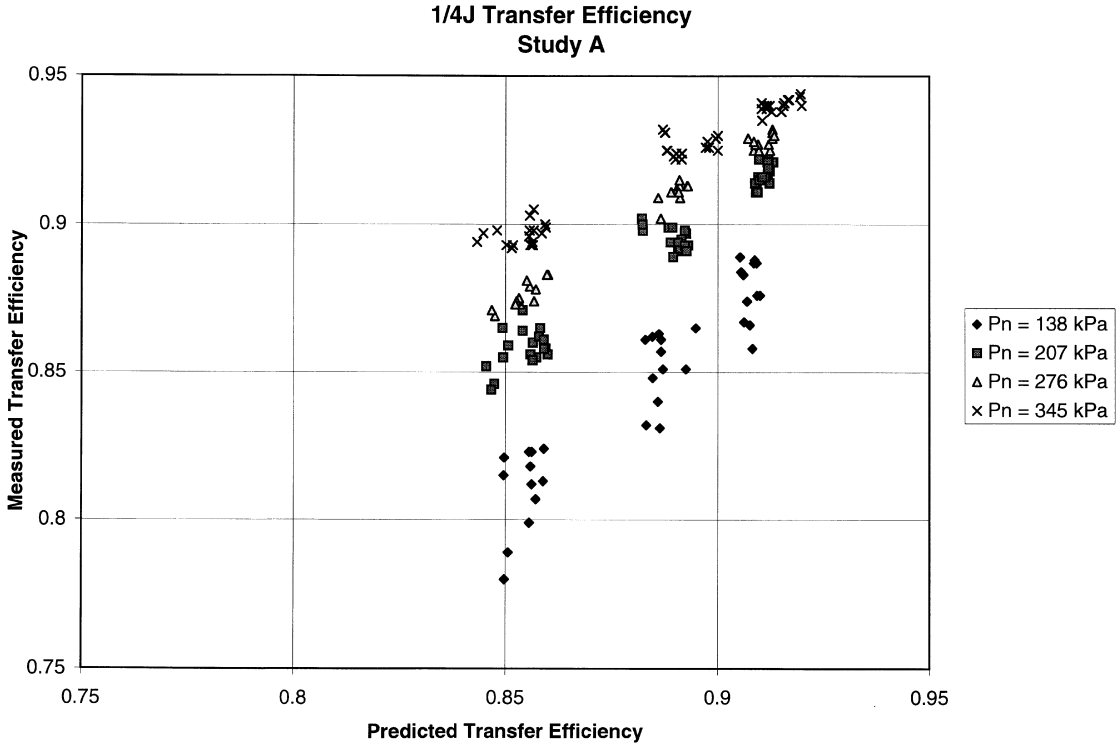


Fig. 5. Measured vs. predicted transfer efficiencies by nozzle pressure for Study A (1/4 J and wind tunnel).

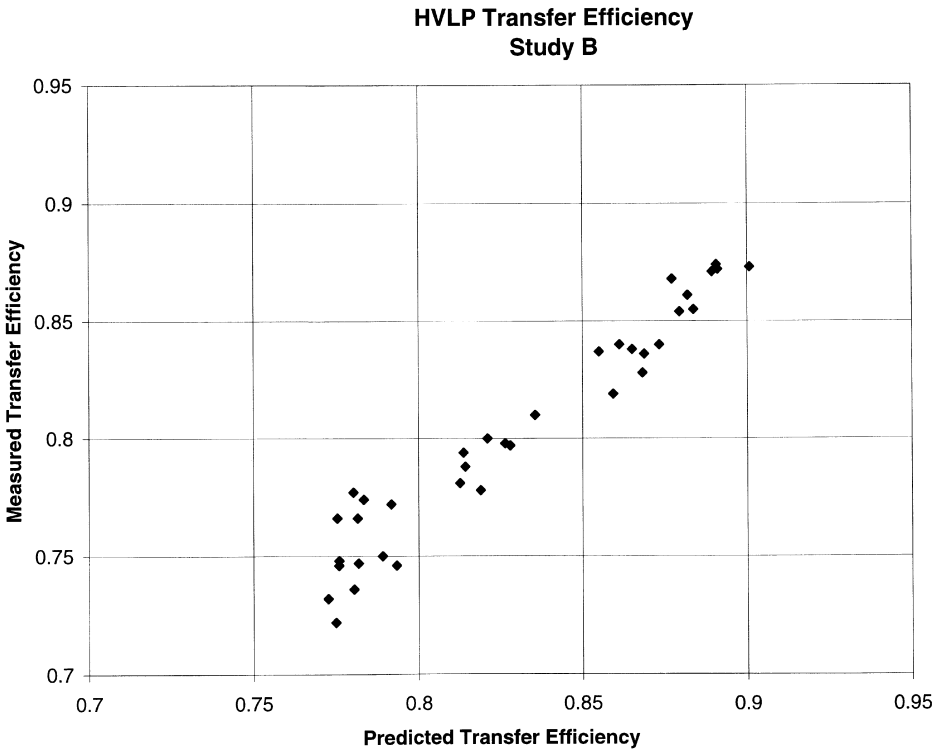


Fig. 6. Measured vs. predicted transfer efficiencies for Study B (HVLP gun and spray-booth).

groups, corresponding to values of the air-to-liquid mass ratio (0.7, 0.9 and 1.3), which essentially determined the predicted transfer efficiency. Figure 6 illustrates the HVLP transfer efficiency data, which showed no dependence on nozzle pressure, but which consistently underestimated the predicted value. Table 5 presents results of least squares regressions of measured vs. predicted transfer efficiency. Study A regressions were based upon nozzle pressure and indicated a tendency for the slope to increase and the intercept to decrease as nozzle pressure diminished. There was no appreciable difference in transfer efficiency observed for either orientation in either study.

## DISCUSSION

The exposure data shown in Fig. 3 suggest that the momentum flux ratio and orientation were good predictors of the dimensionless exposure. The curve fits defined by eq. (14) and eq. (15), and the general trends observed for data from both studies A and B, suggest a general model of the form:

$$\log_{10}\left(\frac{CHUD}{m_o}\right)=\alpha+\Delta\left(\frac{F_g}{F_m}\right)^{\gamma}, \qquad (16)$$

where $\alpha$, $\delta$ and $\gamma$ are constants, depending on geometry and orientation. The absence of Reynold's numbers in the dimensional analysis and the importance of the momentum flux ratio suggests that inertial forces, rather than viscous forces, governed the transport mechanisms. This is reasonable given the high velocities and pressures involved in the studies. In addition, these inertial forces will also drive the turbulent transport. Given the enormous velocity gradients during spraying and the accompanying high generation rates of turbulence kinetic energy in the booth, it is assumed that the results obtained here are relatively insensitive to any realistic variation in turbulence intensity at the inlet to the spray-booth or wind tunnel.

Table 5. Regression analysis: observed vs. predicted transfer efficiency

| Study | Nozzle pressure (kPa) | Slope | 95% C.I. for slope | Intercept | 95% C.I. for intercept | $r^2$ |
|---|---|---|---|---|---|---|
| A | 138 | 1.27 | (1.1, 1.45) | −0.28 | (−0.43, −0.12) | 0.86 |
| A | 207 | 1.02 | (0.96, 1.09) | −0.015 | (−0.07, 0.04) | 0.95 |
| A | 276 | 0.92 | (0.89, 0.97) | 0.09 | (0.06, 0.12) | 0.98 |
| A | 345 | 0.71 | (0.67, 0.75) | 0.29 | (0.25, 0.33) | 0.96 |
| B | 10.4–44.9 | 1.04 | (0.95, 1.13) | −0.06 | (−0.14, 0.01) | 0.94 |

The data shown in Fig. 3 for studies A and B are close but do not coincide. In order for both data sets to collapse onto two curves, one for each orientation, all length scale ratios and momentum flux ratios would have to be the same. As the data in Table 1 indicate, some of these ratios are close, e.g., each mannequin had a $D/H$ ratio of about 0.2 and the ratio of $D$ to the plate width was about 0.32 in both cases. However, the plate width to tunnel width was 0.43, while the comparable value in the spray-booth was 0.56. Various other length scale ratios differed as well, particularly the arm length as a fraction of $D$, and were probably important in accounting for the observed differences.

In addition, the distribution of air velocities in the spray-booth was not as uniform as in the wind tunnel. There tended to be higher velocities on one side of the booth. To account for this, the velocity in the vicinity of the spraying operation was estimated from anemometer measurements rather than from the average booth velocity. It is likely, however, that this nonuniformity of velocity affected the comparability of the two studies as well.

The agreement between measured and predicted transfer efficiencies in study B was good despite a modest negative bias. The dependence on nozzle pressure in study A is more difficult to explain. This could reflect the influence of fan air because in study B the HVLP gun was always operated with fan air on, but in study A, the 1/4 J nozzle had no fan air. Possibly, the fan air produced a more uniform mixing of particles and velocities, which would favor the assumptions invoked in the model. In addition, the 1/4 J nozzle (study A) always operated at sonic velocity and the accompanying rapid expansion of the high-pressure air at the nozzle may have promoted nonuniform particle distributions. Studies (Domnick et al., 1991; Care and Ledoux, 1991) have shown that the radial distribution of droplets within sprays is not uniform. There appears to be a tendency for larger particles to migrate to the periphery of the spray due to their sustained radial velocities relative to smaller droplets. There also appears to be a more peaked velocity distribution at the edges of the spray than predicted by the model.

## CONCLUSIONS

This study suggests that for compressed air spray painting in cross-flow booths, a dimensionless breathing zone concentration was a nonlinear function of the ratio of the momentum flux of air from the spray gun to the momentum flux of air passing through the projected area of the worker's body. The geometrical configuration and orientation of the spraying operation within the booth were also significant determinants of the breathing-zone concentration. The deflection of the spray upstream into the booth airflow, and subsequent recirculation to the worker, was responsible for the elevated breathing-zone concentations in the side orientation.

The model required an estimate of the contaminant generation rate, which is approximated here with a simple impactor model for transfer efficiency. The droplet size distribution, determined from previously published empirical work, worked reasonably well for the HVLP spray gun with the fan-air on, but showed a consistent difference with nozzle pressure for the 1/4 J nozzle at sonic velocities and no fan air.

This study represents an initial step in the construction of more detailed and realistic models for spray painting exposures. Determining the generation rate of material available for exposure and characterizing the airflow field, transporting the contaminant to breathing zone, are the key features of the modeling effort. Important areas requiring consideration include the phase-partitioning question, arbitrary geometry and time-dependent effects, including worker activity. Further research into the overspray generation mechanism is needed as well, particularly information on the spatial distribution of droplet sizes and velocities.

*Acknowledgements*—This work was supported by grant number R01/OH02858 from the U.S. National Institute of Occupational Safety and Health (NIOSH). Its contents are solely the responsibility of the authors and do not necessarily represent the official views of NIOSH.

## REFERENCES

Abramovich, G. N. (1963) *Theory of Turbulent Jets*. MIT Press, Cambridge, Mass.

Baturin, V. V. (1972) *Fundamentals of Industrial Ventilation*. Pergamon Press, Oxford, UK.

Blazicko, B. (1998) *The Evaluation of Momentum Flux to Estimate Exposure from Spray Painting Operations*. MSEE Technical Report, University of North Carolina, Chapel Hill, NC.

Care, I, and Ledoux, M. (1991) Study of an airblast coaxial atomizer experiments and modelisation. In: *Proceedings of the 5th International Conference on Liquid Atomization and Spray Systems*, NTIS pb91–216838, pp. 763–770.

Carlton, G. N. and Flynn, M. R. (1997) A model to estimate worker exposure to spray paint mists. *Appl. Occup. Environ. Hyg.* **12(5),** 375–382.

Carlton, G. N. and Flynn, M. R. (1997) Field evaluation of an empirical–conceptual exposure model. *Appl. Occup. Environ. Hyg.* **12(8),** 555–561.

Domnick, J., Tropea, C. and Xu, T. H. (1991) Measurements in paint sprays using a phase–doppler anemometer. In: *Proceedings of the 5th International Conference on Liquid Atomization and Spray Systems*, NTIS pb91–216838, pp. 129–138.

Dunn, K. (1997) An Investigation of Factors Affecting the Development of an Empirical Conceptual Model for Estimating Spray Paint Exposure in a Cross Draft Spray Booth. MSEE Technical Report, University of North Carolina, Chapel Hill, NC.

Gatano, B. L. (1997) Determination of Transfer Efficiency from an HVLP Spray Gun. MSEE Technical Report, University of North Carolina, Chapel Hill, NC.

Hinds, W. C. (1982) *Aerosol Technology Properties, Behavior and Measurement of Airborne Particles*. John Wiley & Sons, NY, NY.

Kim, K. Y. and Marshall, J. R. (1971) Drop-size dis-

tributions from pneumatic atomizers. *AIChE J.* **17(3),** 575–584.

Kim, T. and Flynn, M. R. (1992) The effect of contaminant source momentum on a worker's breathing zone concentration in a uniform freestream. *Am. Ind. Hyg. Assoc. J.* **53(12),** 757–766.

Kwok, K. (1991) A fundamental study of air spray painting. Ph.D. dissertation, University of Minnesota.

McKernan, J. (1997) Effect of Position and Motion on Personal Exposure in an HVLP Spray Painting Operation. MS Technical Report, University of North Carolina, Chapel Hill, NC.

Schlichting, H. (1979) Boundary Layer Theory. McGraw–Hill, New York, NY.

Tsai, S. C. and Viers, B. (1992) Airblast atomization of viscous newtonian liquids using twin-fluid jet atomizers of various designs. *J. Fluids Engnr.* **114,** 113–118.

White, F. W. (1986) *Fluid Mechanics*. McGraw–Hill, New York, NY.